Neuro-Oncology

Neuro-Oncology 16(1), 38–49, 2014
doi:10.1093/neuonc/not141
Advance Access date 4 December 2013

Tumor targeting using magnetic nanoparticle Hsp70 conjugate in a model of C6 glioma

Maxim A. Shevtsov, Ludmila Y. Yakovleva, Boris P. Nikolaev, Yaroslav Y. Marchenko, Anatolii V. Dobrodumov, Kirill V. Onokhin, Yana S. Onokhina, Sergey A. Selkov, Anastasiia L. Mikhrina, Irina V. Guzhova, Marina G. Martynova, Olga A. Bystrova, Alexander M. Ischenko, and Boris A. Margulis

Institute of Cytology of the Russian Academy of Sciences, St. Petersburg, Russia (M.A.S., K.V.O., I.V.G., M.G.M., O.A.B., B.A.M.); Research Institute of Highly Pure Biopreparations, St. Petersburg, Russia (L.Y.Y., B.P.N., Y.Y.M., A.M.I.); Institute of Macromolecular Compounds of the Russian Academy of Sciences, St. Petersburg, Russia (A.V.D.); D. O. Ott Institute of Obstetrics and Gynecology, Northwestern Division of the Russian Academy of Medical Sciences, St. Petersburg, Russia (Y.S.O., S.A.S.); I. M. Sechenov Institute of Evolutionary Physiology and Biochemistry of the Russian Academy of Sciences, St. Petersburg, Russia (A.L.M.)

Corresponding author: Maxim A. Shevtsov, MD, PhD, Laboratory of Cell Protection Mechanisms, Institute of Cytology of Russian Academy of Sciences, Tikhoretsky Ave. 4, 194064, St. Petersburg, Russia (shevtsov-max@mail.ru).

Background. Superparamagnetic iron oxide nanoparticles (SPIONs), due to their unique magnetic properties, have the ability to function both as magnetic resonance (MR) contrast agents, and can be used for thermotherapy. SPIONs conjugated to the heat shock protein Hsp70 that selectively binds to the CD40 receptor present on glioma cells, could be used for MR contrast enhancement of experimental C6 glioma.

Methods. The magnetic properties of the Hsp70-SPIONs were measured by NMR relaxometry method. The uptake of nanoparticles was assessed on the C6 glioma cells by confocal and electron microscopes. The tumor selectivity of Hsp70-SPIONs being intravenously administered was analyzed in the experimental model of C6 glioma in the MRI scanner.

Results. Hsp70-SPIONs relaxivity corresponded to the properties of negative contrast agents with a hypointensive change of resonance signal in MR imaging. A significant accumulation of the Hsp70-SPIONs but not the non-conjugated nanoparticles was observed by confocal microscopy within C6 cells. Negative contrast tumor enhancement in the T2-weighted MR images was higher in the case of Hsp70-SPIONs in comparison to non-modified SPIONs. Histological analysis of the brain sections confirmed the retention of the Hsp70-SPIONs in the glioma tumor but not in the adjacent normal brain tissues.

Conclusion. The study demonstrated that Hsp70-SPION conjugate intravenously administered in C6 glioma model accumulated in the tumors and enhanced the contrast of their MR images.

Keywords: glioma, Hsp70, magnetic nanoparticles, SPION, targeted delivery.

Superparamagnetic iron oxide nanoparticles (SPIONs) have attracted attention in the past decades due to their possible applications in brain tumor therapy, imaging, or drug delivery.[1,2] Since nanoparticles cross the blood–brain barrier (BBB), they could be applied in the development of novel therapeutic modalities. One of the most promising approaches is based on the application of localized hyperthermia, when magnetic nanoparticles (MNPs) absorb energy from alternating magnetic fields and transform this energy into heat.[3,4] The efficacy of this method was demonstrated in numerous preclinical and clinical studies.[5–9] Recently, Maier-Hauff et al,[10] in a single-arm phase II study of intratumoral thermotherapy combined with external beam radiotherapy in patients with recurrent glioblastoma, showed significant increase in overall survival (up to 23.2 mo) in comparison with historical control of 14.6 months reported by Stupp et al.[11]

Currently, the delivery of MNPs is based on a direct intratumoral injection, which limits the clinical application of this method.[10] Further improvement of tumor targeting by the SPIONs requires a special surface coating, which can provide the specificity of SPION delivery to the tumor cells in vivo.[12] Thus, conjugation to the purified antibody that selectively binds to the epidermal growth factor receptor deletion mutant (EGFRvIII) present on glioblastoma cells significantly elevated the efficacy of the accumulation of MNPs in the tumor site.[13] In the elegant study by Basel et al,[7] the authors used cytotherapy-directed hyperthermia when MNPs were loaded into monocyte/macrophage-like cells, which have

Received 20 May 2013; accepted 29 July 2013

been shown to specifically migrate into the tumor. Further studies demonstrated that the therapeutic efficacy of local hyperthermia could be increased by combination with other methods, including use of various anticancer drugs.[6,14] Thus, Fe_3O_4 MNPs combined with chemotherapy and hyperthermia could overcome the multidrug resistance in an in vivo model of leukemia.[6]

Earlier we developed MNPs with a size <100 nm that were considered to have low toxicity.[15] For elevating the efficacy of tumor targeting, we conjugated MNPs with epidermal growth factor (EGF), which increased the selectivity of the MNP-EGF accumulation in cancer cells in a melanoma mouse model.[15] The developed formulation of the MNP-EGF conjugates was characterized by the coefficients of magnetic relaxation efficacy (R_1, R_2, R_2^*), which were close to the characteristics for the negative contrast agents for MRI. This resulted in the generation of a strong hypointense T_2-weighted contrast on MRI.[15] In the present study, for brain tumor targeting, we decided to use recombinant heat shock protein (Hsp)70 covalently conjugated to the surface of the SPIONs. Several reasons were taken into consideration for the application of Hsp70. First was the possibility of selective brain tumor targeting due to the overexpression by the glioma Hsp70 cell receptors. Previously, various receptors to Hsp70 have been identified, including CD91, lectin-type oxidized low-density lipoprotein receptor 1 (LOX-1), Toll-like receptors (TLR-2/TLR-4), and CD40.[16–18] In several studies it was observed that on the cell surface of glioma cells, CD40 was highly expressed in comparison with the surrounding normal tissues.[19–21] The prevailing expression of CD40 in the glioma can cause the accumulation of the SPIONs conjugated with Hsp70 in the tumor site. The second reason for the application of Hsp70 was its immunomodulatory activity, as Hsp70 is involved in the generation of adaptive and innate antitumor immune responses.[22] This immunomodulatory function could be used for augmentation of the immune response that is generated by the localized hyperthermia of the tumor. Previously, Ito et al[23] demonstrated in a model of melanoma the therapeutic potential of local intratumoral delivery of Hsp70 combined with magnetic nanoliposome-based hyperthermia.

In the current study, in the model of the intracranial C6 glioma, we demonstrate the possibility of glioma targeting by Hsp70-SPION conjugates that could be intravenously injected.

Materials and Methods

Preparation of Recombinant Hsp70

Recombinant human Hsp70 was prepared from *Escherichia coli* transformed with a pMSHsp70 plasmid. Hsp70 was purified by anion exchange chromatography using diethylaminoethanol-sepharose (GE Healthcare) followed by ATP-affinity chromatography on ATP-agarose (Sigma). Endotoxin was depleted by polymixin B-sepharose endotoxin removing gel (Sigma). Quantitation of endotoxin was performed using the *Limulus amoebocyte* lysate assay (QCL-1000, Cambrex Bio Science). The resulting endotoxin content was below 0.1 endotoxin unit per milligram. For the analysis of Hsp70 uptake, in both in vitro and in vivo experiments the chaperone was conjugated with Alexa Fluor 555 (Invitrogen) according to the manufacturer's protocol.

Synthesis of Iron Oxide MNPs

SPIONs were prepared by coprecipitation in alkaline media at 80°C.[24] Iron salts $FeSO_4$ and $FeCl_3$ at Fe2+/Fe3+ ratio 1:2 were dissolved in distilled water with addition of some salt. The precipitation was performed by the dropwise addition of NH_4OH to the iron salt solution under nitrogen gaseous atmosphere with vigorous stirring. The magnetite formation follows the reaction

$$2\,Fe(+3) + Fe(+2) + 8OH^- \rightarrow Fe_3O_4 + 4\,H_2O.$$

Magnetic crystal formation was completed by stirring the stock solution after 5 min. To stabilize suspension for storage, the particles were coated by low molecular dextran (molecular weight, 10 kD; Sigma). For best surface modification, ultrasound sonication at 22 kHz was applied. The stock solution of MNPs was washed and size-fractionated to 4 fractions by centrifugation and ultrafiltration using fiber membranes (0.2 μm; Millipore). The finest fraction of nanoparticles was stored in water at 4°C for analysis and further conjugation.

Magnetic Hsp70 Conjugate Synthesis

The synthesis of magnetic conjugates of Hsp70 with SPIONs was carried out in accordance with the scheme shown in Figure 1A. Dextran-coated MNPs were crosslinked with epichlorohydrin and aminated. MNPs were suspended in phosphate buffered saline (PBS) solution with 60 μg of Hsp70, and conjugation was carried out for 1 h at 20°C in a shaker. Activated by water-soluble carbodiimide, dextran was coupled to carboxyl groups of Hsp70 protein, producing magnetic conjugate. The size of SPIONs or Hsp70-SPIONs was assessed using atomic force microscopy (AFM). Briefly, nanoparticles in 10 μL of the sample were placed on the microscope slide and were allowed to air dry. Samples were then processed with AFM on an NTEGRA Prima scanning probe microscope (NT-MDT). Closed-loop feedback semicontact mode was used at a rate of 0.6 Hz. Scanning started from the 50-μm area, going down to 5 μm. The images obtained were analyzed with NT-MDT image analysis software v2.2. At least 25 individual particles were measured from 3 different positions, and the average diameter was reported. The surface morphology of the sample was observed in a large-scale scanning area of 700 nm × 700 nm and 1000 × 1000 pixels.

The Hsp70 content in conjugate samples was measured by ELISA. The biological activity of Hsp70 in the conjugate was assessed by the chaperone ELISA and found not to be changed by the conjugation with SPIONs.[25] The magnetic Hsp70 conjugate samples were analyzed for content of total Fe by spectrophotometry of thiocyanate Fe(+3) complex obtained after HNO_3 dissolution.

Cells

The C6 rat glioma cell line was obtained from the Russian cell culture collection of the Institute of Cytology in St Petersburg. C6 cells were grown in Dulbecco's modified Eagle's medium/F12 supplemented with 10% fetal bovine serum, 2 mM L-glutamine, and antibiotics (100 U/mL penicillin G and 0.1 mg/mL streptomycin). Cells were grown in a CO_2 incubator in an atmosphere with 6% CO_2 and 90% humidity. For in vivo experiments, C6 cells were also infected with recombinant lentivirus vectors (including LVTHM, which expresses green fluorescent protein [GFP]), and C6-GFP+ cells were analyzed with the aid of flow cytometry (Cytomics FC500, Beckman Coulter). Before experiments, cells were harvested in log phase of growth, and their viability was determined by 0.4% trypan blue exclusion.

Model of Intracranial C6 Glioma in Rats

Before being mounted in a stereotactic frame (David Kopf Instruments), male Wistar rats (250–300 g) were anesthetized with 10 mg tiletamine hydrochloride and zolazepam (Zoletyl-100, Virbac) and 0.2 mL 2% xylazinum hydrochloride (Rometar, Bioveta) intraperitoneally. A burr hole was made 1 mm posterior to the bregma and 3 mm to the right of the midline. Rat C6 glioma (10^6) cells in 10 μL PBS were injected 3 mm below

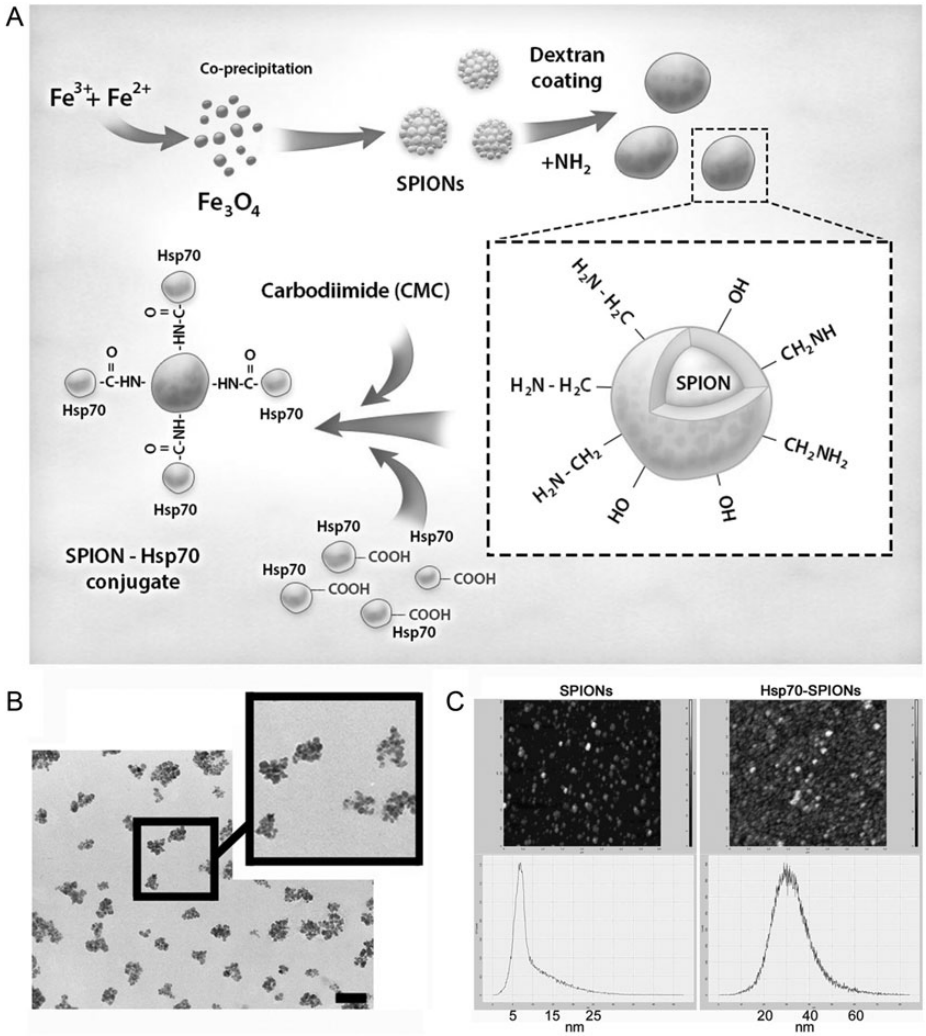

Fig. 1. The preparation and microscopic image of Hsp70-SPION conjugate. (A) Scheme of synthesis of Hsp70-SPION conjugates. (B) Transmission electron microscopy image of Hsp70-SPION conjugates. Scale bar, 1 μm. (C) Atomic force microscopy of the SPIONs and Hsp70-SPION conjugates.

the cortical surface using a Hamilton microsyringe. Stereotactic coordinates corresponded to the nucleus caudatus dexter (per the stereotactic atlas of Pellegrino). All animal experiments were approved by the local ethical committee.

Magnetic Relaxometry and MRI Study

Nuclear magnetic resonance (NMR) spectra and magnetic relaxation times T_1, T_2, T_2^* were measured with the help of an NMR spectrometer (CXP-300, Bruker) in a magnetic field of 7.1 T. The NMR spectra were recorded by Fourier transform of one-pulse induction decay. T_2^* was calculated from line width at half height. To estimate magnetic relaxation times, inversion recovery and Carr-Purcell-Meiboom-Gill pulse sequences were applied. Proton relaxation times were studied dependent on the concentration of magnetic Hsp70 conjugates in buffer solution in 5-mm tubes. The coefficients of relaxation efficiency R_1, R_2, R_2^* (relaxivity) were determined from the slopes of concentration plots of inverse times of magnetic relaxation.

The rat and gel phantom images were acquired with the help of a Bruker Avance II NMR spectrometer equipped with a microtomographic accessory at a magnetic field of 11 T. The measurements were carried out using gradient echo fast imaging and multiscan-multiecho imaging. The T_1, T_2-weighted images were obtained under the scanning regimes of rapid acquisition with relaxation enhancement (RARE) – T_1 and Turbo-RARE-T_2 . A series of transverse and coronal sections of tumor were acquired after intravenous injection of Hsp70-SPION conjugates at different times and under different regimes of acquisition.

Assessment of Distribution of Hsp70 in C6 Glioma

On the 20th day following intracranial implantation of the C6 glioma cells or C6 cells labeled with GFP, the Hsp70 – Alexa Fluor 555 conjugate was i.v. injected into the tail vein (5 mg/kg in 200 μL of saline solution, for 3 animals in each group). Twenty-four hours after the protein injection, animals were sacrificed, brains were extracted and fixed in 4% paraformaldehyde (PFA), and serial frozen sections were obtained. Nuclei were stained with 4′,6′-diamidino-2-phenylindole (DAPI). Additionally, the brain sections were stained with anti-CD40 fluorescein isothiocyanate (FITC) – conjugated monoclonal antibodies (1/100; BD Biosciences). Immunofluorescence images were captured with a Leica TCS SP5 confocal system.

Assessment of Hsp70-SPION Conjugate Uptake by C6 Cells

C6 glioma cells were allowed to settle on glass slides coated with poly-L-lysine. Cells were incubated with PBS, SPIONs (0.05 mg/mL), or

Hsp70-SPION conjugates (0.05 mg/mL) in cell culture medium for 1, 6, 12, and 24 h at 37°C, 6% CO_2. Following incubation with nanoparticles, cells were excessively washed and fixed with 4% PFA. Nuclei were stained with DAPI. Immunofluorescence images were captured with a Leica TCS SP5 confocal system at 488 nm (Ar/Kr) and 405 nm on a Leica DM IRBE microscope. We also analyzed the role of CD40 receptor in the uptake of Hsp70-SPION complexes by the C6 cells. Cells were incubated with blocking anti-CD40 monoclonal antibodies (dilution 1:100; BD Biosciences) for 2 h. Following incubation with antibodies, C6 cells were incubated with Hsp70-SPION conjugates for 1, 6, 12, and 24 h at 37°C, 6% CO_2, then washed and fixed with 4% PFA. The internalization of the conjugates was assessed with confocal microscopy.

For evaluation of the precise intracellular localization of the nanoparticles, electron microscopy was performed. Experiments were conducted as follows: C6 cells were exposed to SPIONs or Hsp70-SPIONs at a concentration of 0.05 mg/mL in cell culture medium for 24 h at 37°C, 6% CO_2. Following incubation with nanoparticles, probes were centrifuged and the pellet was postfixed with 1% osmium tetroxide in 0.1 M cacodylate buffer for 30 min, dehydrated in a graded series of ethanol dilutions, and embedded in Durcupan (Fluka). After polymerization, serial ultrathin sections from the pellet were cut on an Ultracut ultramicrotome (Reichert-Jung) and collected on Nickel 200 mesh square grids. Sections were counterstained with lead citrate and examined with a JEM1200EX electron microscope (Jeol). Additionally we performed immunogold labeling of the C6 cells by monoclonal anti-CD40 antibodies (BD Biosciences). For immunocytochemical examination, ultrathin sections mounted on nickel grids were first treated with hydrogen peroxide for 20 min to loosen the resin. Three washes in PBS for 2 min each were followed by incubation with anti-CD40 monoclonal antibodies diluted 1:100 in 0.05 M Tris-HCl buffer, pH 7.4, containing 1% bovine serum albumin and 0.1% cold water fish gelatin overnight, at 4°C in a moist chamber. Gold-conjugated (10 nm) goat anti-mouse immunoglobulin G (Sigma) diluted 1:10 was used as secondary antibody, and sections were incubated for 1 h at room temperature. For the control, the primary antibody was omitted or replaced by irrelevant antibodies.

Immunofluorescence Analysis of Nanoparticle Uptake In vivo

Twenty-four hours following i.v. injection of Hsp70-SPIONs or SPIONs, animals were sacrificed with CO_2 and transcardially perfused with PBS for 15 min (20 mL/min), followed by 4% PFA (in 0.1 M phosphate buffer, pH 7.4) fixation for 15 min (20 mL/min). Tumor tissue samples were harvested into Tissue-Tek compound for sectioning and stored at −80°C. Serial 7-μm frozen sections were stained with DAPI. Sections were analyzed on the confocal microscope in reflected-light laser scanning with a Leica TCS SP5 confocal system.

Statistical Analysis

Continuous variables were compared using a paired Student's test. Statistical significance was determined at the $P < .05$ level. A 2-tailed Mann–Whitney log-rank test was used to compare study and control groups.

Results

Magnetic Relaxometry and Size Analysis of Hsp70-SPION Conjugate

The prepared suspensions of SPIONs and their conjugates with different iron contents were investigated by magnetic relaxometry and AFM. The size of the nanoparticles was determined by AFM on solid surfaces after drying. The microscopy data indicated the existence of single spherical particles with diameters ranging from 15 to 25 nm (SPIONs) and mean particle size of 20 nm, respectively (Fig. 1C). For Hsp70-SPION conjugates, the size ranged from 20 to 40 nm, and the mean size was 35 nm (Fig. 1B and C). Also, some clusters were observed with a mean size of about 100 nm. Fresh samples of suspensions were transparent brown solutions that were stable at 4°C storage. Magnetic relaxometry analysis showed the paramagnetic property of the suspension. The addition of SPIONs or conjugates into distilled water caused strong decreases of relaxation time T_1, T_2 of water protons from 3 s to 100–300 ms. The decrease of relaxation time correlated with the growth of SPION concentrations. The reciprocals of magnetic relaxation times R_1, R_2 were estimated from a linear fit of logarithmic echo amplitude versus spin echo time (Fig. 2). The commercial MR contrast agent fluid MAG-DX (Chemicell) was used for comparative control. The R_1, R_2, R_2^* relaxivity values of synthesized SPION-Hsp70 conjugates were 0.37, 113, and 230 $mM^{-1}\,s^{-1}$, respectively. The range of relaxivity was no worse than for MAG-DX and corresponded to properties of negative contrast agents. These results suggest the strong relaxation efficiency of magnetic Hsp70 conjugates in aqueous dispersions.

The action of the strong magnetic field of 7.1 T on aggregation of Hsp70-SPIONs was investigated by relaxation study in dynamics. Proton magnetic relaxation rates r1, r2, r2* were recorded after inserting the samples with conjugated and nonconjugated SPIONs into a uniform magnetic field of the NMR spectrometer for long periods of time. NMR acquisition was performed step by step by applying impulse sequences at different time points. A 2-phase behavior of the magnetic relaxation rates of water protons r1, r2, r2* time in suspensions of MNPs was observed. The first phase of the fall of the rate of magnetic relaxation occurred immediately after inserting the sample into the magnetic field. This stage of transition to equilibrium lasted for about 3 h. The second phase was characterized by almost constant values of the magnetic relaxation rates for periods from 3 h to 20 h. Further observation did not reveal any changes in relaxation behavior. The largest drop in relaxation rate (almost 2-fold) was observed when measuring the value of r2* (Fig. 2).The similar plots for r1, r2 are not shown for their resemblance in general form. After a long prehistory (20 h) in the 7.1-T magnetic field, the rate of magnetic relaxation of SPIONs and Hsp70-SPION conjugates remained constant in time. The stability of the magnetic Hsp70 conjugate was shown to be sufficient for further MRI studies of tumor-bearing rats.

The magnitude of magnetic relaxation rate of nanoparticle conjugates matches well with their appreciable contrast manifestation in a phantom study made by MRI. Representative images of phantom agar-agar samples loaded by magnetic Hsp70 conjugates at various Fe concentrations are shown in Fig. 2B. The signal intensity of images decreased with the growth of iron oxide in gel. The highest contrast was achieved in T_2-weighted and gradient spin echo regimes in accordance with the strong influence of T_2–outer sphere mechanism relaxation. These relaxation measurements provide evidence that conjugation of nanoparticles with Hsp70 through a carbodiimide linker does not interfere with the nanocrystal structure of the magnetite core. The dextran surface prevents the magnetic core of the nanoparticles from the chemical transformation into a diamagnetic state. The ratio of the relaxation efficiency

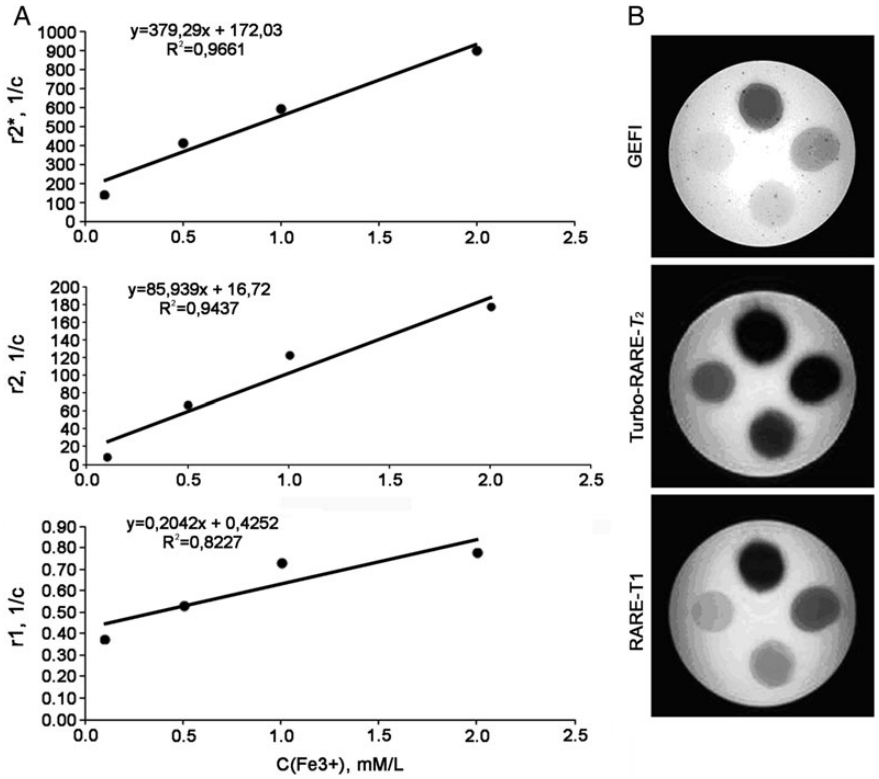

Fig. 2. The magnetic contrast study of Hsp70-SPION conjugate in vitro. (A) Relationship of magnetic relaxation rate r_2^*, r_2 and r_1 of water protons in Hsp70-SPION conjugate dispersion vs Fe concentration at 20°C. (B) MR transverse images of agar phantom loaded with Hsp70-SPION conjugates in concentration (anticlockwise) 0.1, 0.2, 0.4, 0.8% obtained under gradient echo fast imaging (GEFI), rapid acquisition with relaxation enhancement (RARE)–T_1 and Turbo-RARE-T_2 scanning regimes.

coefficient R_2/R_1 ranges from several tens to hundreds, which is the basis for regarding the synthesized conjugates of Hsp70 as powerful negative contrast agents.

Accumulation of Hsp70 in the CD40+ C6 Glioma Cells

Assessment of the intratumoral accumulation of Hsp70 was performed in the case of the i.v. injection of the fluorochrome-labeled protein. Twenty-four hours after the infusion of Hsp70–Alexa Fluor 555 (5 mg/kg in saline solution), the protein could be observed in the tumor site (Fig. 3A). Hsp70 was distributed throughout the glioma accumulating within the cytoplasm and the nucleus environment. In some cells, Hsp70 appeared to form aggregates in the cytoplasm. For the confirmation of the incorporation of the Hsp70 inside C6 glioma cells, the latter were labeled with GFP and inoculated into the rat brain. The subsequent i.v. injection of Hsp70–Alexa Fluor 555 confirmed the accumulation of the protein inside the C6 cells (Fig. 3B). The Hsp70 accumulated within the cytoplasm of the GFP+ cells. Following the assessment of intratumoral distribution of Hsp70, we analyzed the possible accumulation of the labeled protein in the CD40+ glioma cells, as CD40 was described as a receptor for Hsp70.[16,26] Immunofluorescence images of the C6 tumor show the presence of the CD40+ cells throughout the tumor (Fig. 3C). When we stained the frozen tumor sections of the animals being i.v. injected with Hsp70–Alexa Fluor 555 with anti-CD40 antibodies, we were able to confirm the accumulation of Hsp70 inside the CD40+ cells (Fig. 3D).

Confirmation of Hsp70–SPION Conjugates Binding to C6 Glioma Cells

Rat C6 glioma cells were incubated with control (PBS), SPIONs (0.05 mg/mL), and Hsp70-SPIONs (0.05 mg/mL) for 1, 6, 12, and 24 h. At first, the cell viability with 0.4% trypan blue was assessed for all of the incubation times with nanoparticles. There was no significant toxicity found within C6 cells after treatment with SPIONs or Hsp70-SPIONs. Following viability assessment, the inclusion of nanoparticles inside C6 cells was analyzed with the help of confocal microscopy (Fig. 4A–C). SPIONs or Hsp70-SPION conjugates gradually deposited onto C6 glioma cells and passed through the plasma membrane. Nanoparticles appeared to be present within the cytoplasm and to surround the nucleus. The particles did not seem to penetrate into the nucleus, instead forming coarse aggregates within the cytoplasm; more aggregates were detected in the cytoplasm at 24 h. Intriguingly, the quantity of nanoparticles within the cells was higher in the case of Hsp70-SPIONs than in nonconjugated SPIONs. The cytoplasm of C6 cells incubated with Hsp70 conjugates was completely filled with magnetic

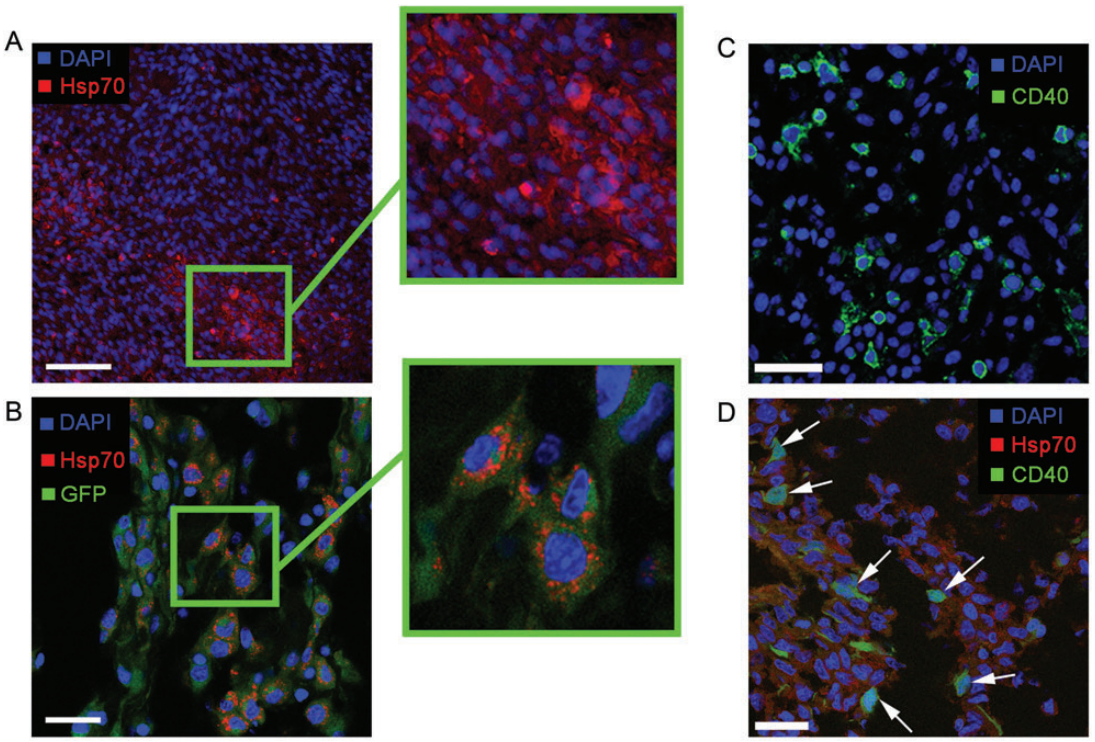

Fig. 3. Accumulation of Hsp70 in C6 glioma cells in vivo. (A) Fluorochrome-labeled (Alexa Fluor 555) Hsp70 was infused intravenously (5 mg/kg) in the tumor-bearing animal on the 20th day following tumor implantation. After 18 h the animal was dissected and assessed for the presence of the labeled chaperone inside tumor cells. Sections were stained with 4′,6′-diamidino-2-phenylindole (DAPI; blue). The labeled Hsp70 (red) accumulated inside the cytoplasm of tumor cells. Scale bar, 75 μm. (B) For confirmation of the localization of exogenous Hsp70 inside glioma cells, the latter were infected with GFP (green). In the same set of experiments, we assessed the distribution of i.v. injected Hsp70–Alexa Fluor 555 protein inside the glioma. The protein accumulated inside the GFP+ C6 cells as red aggregates within the cytoplasm. Scale bar, 25 μm. (C) Immunofluoresence image of C6 glioma tissue section with CD40+ cells detected by FITC-conjugated monoclonal antibodies (green). Nucleus was stained with DAPI (blue). Scale bar, 20 μm. (D) Immunofluorescence image of C6 glioma with CD40+ cells detected by FITC-conjugated monoclonal antibodies (green; shown by white solid arrows). The fluorochrome labeled Hsp70–Alexa Fluor 555 is localized within the cell cytoplasm (red). Nuclei were stained with DAPI (blue). Scale bar, 25 μm.

nanoparticles (Fig. 4C). Electron microscopy images show the nanoparticles containing vesicles within the cytoplasm of the C6 cells incubated with SPIONs or Hsp70-SPIONs (Fig. 4D and F). In a few cases we observed the adsorbed particles on the cell surface, which is a prerequisite for cell internalization. In the case of the Hsp70-SPIONs, we observed the massive presence within the cytoplasm of aggregates that were not surrounded by the membrane (Fig. 4E).Visual examination of the different cell samples demonstrated endosomes containing particles not included in the endosomes in the case of the Hsp70 conjugates. Immunogold labeling with anti-CD40 monoclonal antibodies demonstrated the presence of the Hsp70-SPIONs inside the membrane structures containing CD40 receptor (Fig. 4H). The role of CD40 receptor in the internalization of the Hsp70-SPION conjugates was confirmed with blocking anti-CD40 receptors. When the anti-CD40 antibodies were applied, the significantly reduced uptake of the Hsp70-SPIONs was observed (Fig. 4G).

In control cells containing no nanoparticles, there were few endosomes, indicating that the C6 cells were not phagocytically activated; no electron-positive granules were found inside the endosomes in the control cells (data not shown).

Distribution of the Hsp70-SPION Conjugates in a C6 Glioma Model

Animals on the 20th day after tumor inoculation were divided into 4 groups (3 animals each) according to the subsequent i.v. treatment with nanoparticles: (i) a control group with PBS solution treatment, (ii) SPIONs (0.15 mg/mL, 200 μL), (iii) Hsp70-SPIONs (0.15 mg/mL, 200 μL), and (iv) Hsp70-SPIONs (0.15 mg/mL, 200 μL) with the preliminary injection of Hsp70 (5.0 mg/kg, 24 h before the infusion of nanoparticles). MR scanning was performed 24 h after infusion to determine localization and relaxivity times of the nanoparticles administered (Fig. 5). Intravenous infusions of the Hsp70-SPIONs or nonconjugated SPIONs were safe, as all animals survived the procedures and showed no signs of the toxicity. In the control group of animals without particle treatment, the tumor could be observed on the MR scans with different patterns of growth, including cerebrospinal fluid dissemination into the ventricles. The glioma was characterized by the hypointense signal in the T_1-weighted imaging and hyperintense in the T_2-weighted regimen (Fig. 5A). After MNP infusion, the most significant change in contrast was observed in the tumor on T_2-weighted images. Following i.v. infusion of the SPIONs,

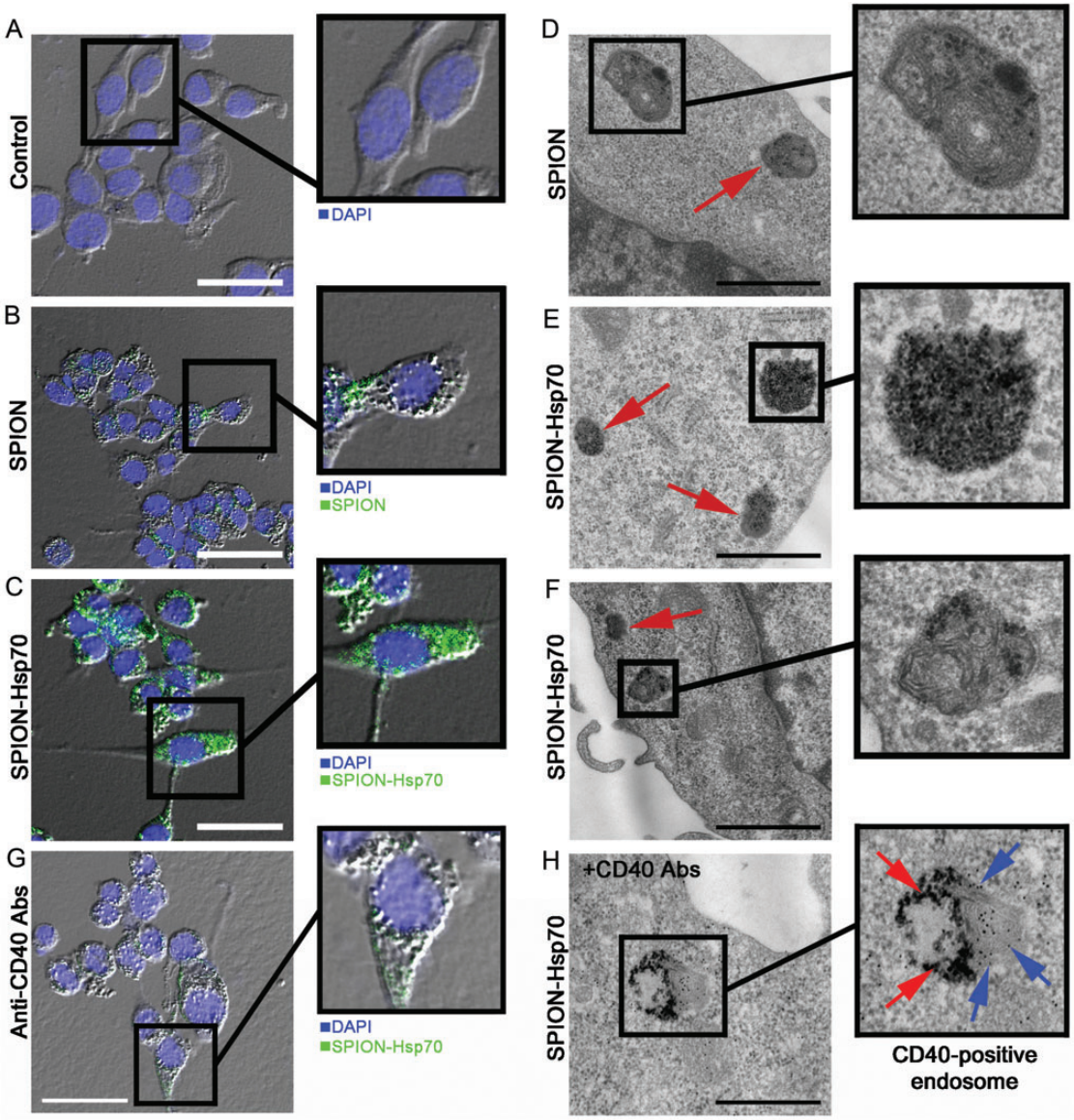

Fig. 4. Fluorescent and transmission electron microscopy images of C6 glioma cells in vitro. (A) Control C6 cells and (B) cells incubated in slide chambers for 24 h with SPIONs (50 μg/mL) or (C) cells incubated with Hsp70-SPION conjugates (50 μg/mL) were fixed with 4% PFA, stained with 4′,6′-diamidino-2-phenylindole (DAPI). Images of cell nuclei (blue) and nanoparticles (green) were acquired sequentially. Nanoparticles appear as green dots or larger coarse aggregates inside the cytoplasm. Scale bar, 25 μm. (D) Electron microscopy images of C6 cells incubated with SPIONs (50 μg/mL) for 24 h. Nanoparticles within the cytoplasm of C6 cells as electron-positive inclusions in the membranous structures are shown by red arrow. Scale bar, 1 μm. (E) Hsp70-SPION conjugates presented as electron-positive inclusions in nonmembranous structures and (F) endosomes within the cytoplasm. Scale bar, 1 μm. (G) Fluorescent image of C6 glioma cells incubated with Hsp70-SPION conjugates (50 μg/mL) for 24 h following treatment with blocking anti-CD40 antibodies. Scale bar, 25 μm. (H) Immunocytochemistry of C6 cell stained with anti-CD40 antibodies. The presence of Hsp70-SPION conjugates (red arrows) inside the CD40+ (blue arrows) membrane structures could be shown. Scale bar, 500 nm.

after 24 h there was a decrease of the T_2 relaxivity time in comparison with the control animals ($P < .05$; Fig. 5B). As can be seen from experiment, a 10% reduction of the transverse relaxation time T_2 was accompanied by the growth of image contrast due to the darkening of sites of MNP accumulation. Application of the Hsp70-SPIONs further reduced the relaxation time in the T_2-weighted regimen, and numerous zones of conjugate aggregates could be observed as areas of signal decrease (especially in the fast low angle shot regimen; $P < .001$; Fig. 5C). On the subsequent postmortem fluorescence images of the brain sections in reflecting-laser light scanning, we confirmed the accumulation of the Hsp70-SPIONs in the glioma tumor. Conjugates appeared to localize within the cytoplasm surrounding the nucleus (Fig. 5, right column). Hsp70-SPIONs not only formed the aggregates within the cells but also were present in the extracellular space. Visual examination discovered more nanoparticles in the case of the Hsp70 conjugate

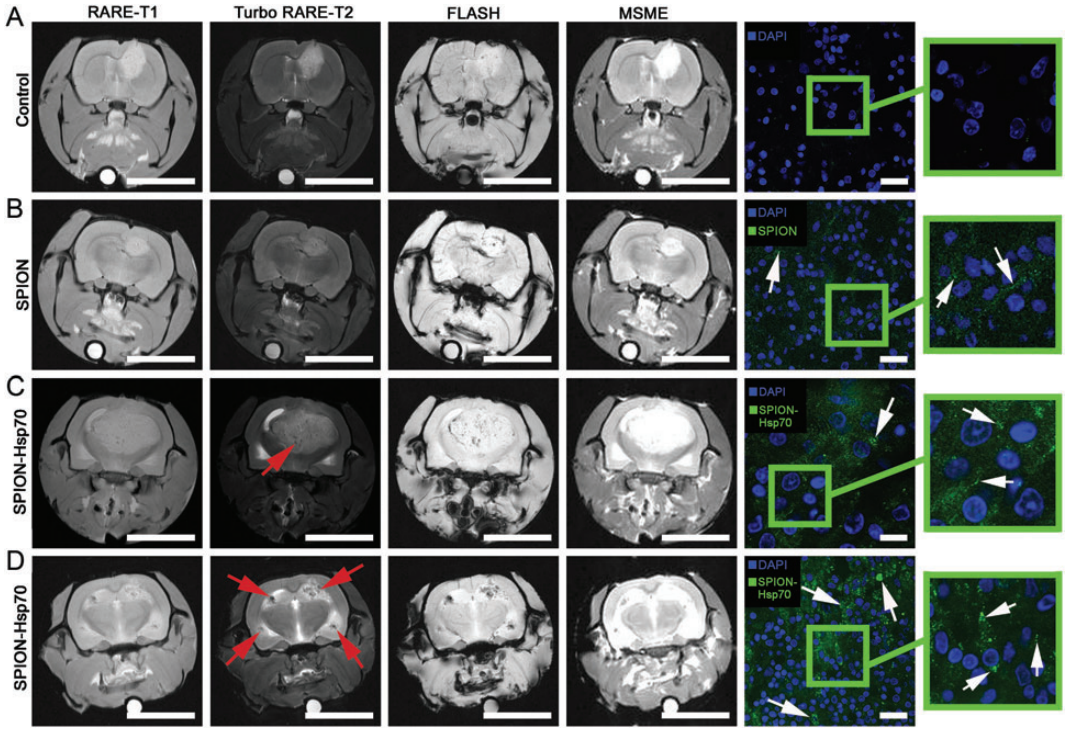

Fig. 5. MRIs of (A) C6 glioma for control, (B) SPIONs i.v. injected, (C) Hsp70-SPION conjugates i.v. infused, and (D) the infusion of Hsp70-SPIONs following preliminary injection of Hsp70. Images were taken following 24 h after nanoparticle infusion at different acquisition regimes: RARE-T1, Turbo-RARE-T2, fast low angle shot MRI (FLASH), and multiscan-multiecho (MSME). Scale bar, 1 cm. Red solid arrows point to the zones of "darkening" inside the glioma that correspond to the nanoparticle accumulation. Following assessment on MR scanner, the brains were extracted, dissected, stained by 4′,6′-diamidino-2-phenylindole (DAPI; blue), and analyzed for nanoparticle presence with the help of confocal microscopy. Nanoparticles appear as green dots or larger aggregates (shown by white solid arrows) within the cytoplasm and in the extracellular space. Scale bar, 25 μm.

application than in the case of nonconjugated SPIONs. The Hsp70 receptor saturation by the i.v. injection of the purified Hsp70 dramatically increased the level of the Hsp70-SPIONs in the tumor (Fig. 5D). Conjugates on the MR T_2-weighted scans appeared as negative contrast "dark" zones and could thus reveal that the tumor was <1 mm in diameter. As observed on T_2-weighted images, the "dark" core inside the tumor could be attributed to the necrotic area. For the differential diagnosis between the specific accumulation of the nanoparticles inside the glioma and tumor necrosis, we applied contrast solution (1.0 mL of 1.0 mmol/mL; Gadovist) for animal #2 from the 4th group. Before mounting the animal in the MR scanner, we i.v. injected Gadovist into the tail vein. Previously it was reported that on T_1-weighted gadolinium (Gd)-enhanced images the tumor necrotic core shows hyperintensities due to the disruption of the BBB.[27] In our study on the subsequent Gd-enhanced T_1-weighted images, we observed only a slight increase in contrast, although the tumor zone remained hypointensive, which indicated the accumulation of Hsp70-SPIONs inside the tumor (Fig. 6).

Discussion

The acquired results of the study of synthesized magnetic conjugates of Hsp70 indicate that conjugates appear as small biocompatible nanoparticles with high magnetic moments. The measured magnetic relaxation times T_1, T_2, T_2^* in aqueous Hsp70-SPION conjugate suspensions are in close relation to the values of initial iron oxide nanoparticles (Figs 1 and 2). Acceleration of magnetic relaxation of water protons in suspensions follows from spatial distribution of magnetic field induced by SPION cores. All absolute values of T_1, T_2, T_2^* and the ratio of T_2/T_1, T_2/T_2 correspond to the magnetic properties of commercially available negative contrast agents, such as CombiDex and Feraheme, which lead to decreased MRI signals. The relaxivity of conjugate Hsp70-SPION calculated from concentration dependencies is comparable to previously reported data of iron oxide nanoparticles conjugated with EGF, vascular endothelial growth factor receptor–targeted antibodies, transferin, aptamers, receptor active peptides, and other bioligands.[15,28]

The negative contrast agents are known to reduce magnetic relaxation times, which results in a hypointensive change of resonance signal in MR scanning. The observed short times of magnetic relaxation of water protons in the presence of magnetic Hsp70 conjugates are due to the intense relaxation of spins in an inhomogeneous magnetic field induced by the magnetic nuclei of superparamagnetic magnetite nanoparticles in conjugate. The diffusion of water molecules around the magnetic centers leads to the partial averaging of local magnetic fields experienced by a spin during the precession in the magnetic field of the spectrometer. In the approximation of the total diffusion averaging, one can expect a strong deviation of the ratio T_2/T_1 of 1. The data demonstrate the performance of relationship $T_2/T_1 > 1$ and $T_2^* > T_2$, which is consistent with the mechanism of the inhomogeneous line broadening due to the strong interference of the magnetic field induced by MNPs. In accordance with the diffusion

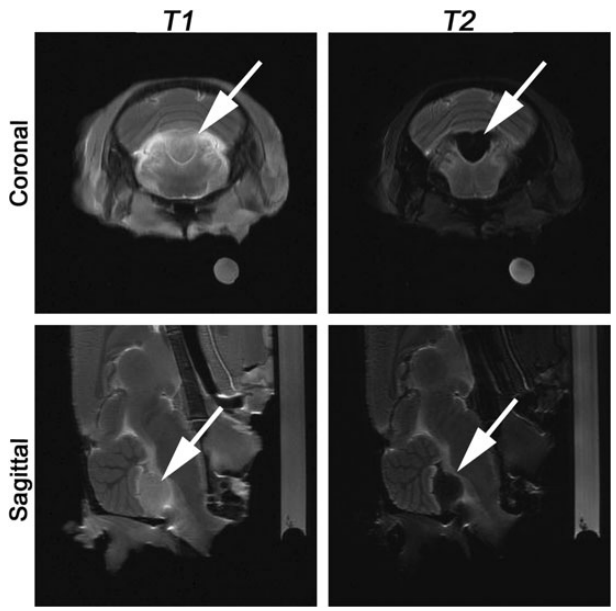

Fig. 6. MRIs of animal #2. Following i.v. infusion of Hsp70 (5 mg/kg), the Hsp70-SPION conjugates (150 μg/kg) were i.v. injected. Before mounting the animal in the head coil i.v., we injected contrast agent (Gadovist, 1.0 mmol/mL, 1 mL). The T_1- and T_2-weighted coronal and sagittal brain sections are presented. Red solid arrows point to the location of the C6 tumor. The accumulation of nanoparticles appears as a "dark" core at the T_2-weighted regimen. On the Gd-enhanced T_1-weighted images, only the slight increase in contrast in the tumor zone is observed.

mechanism of relaxation of the MNPs, the reduction of the relaxation efficiency must be related to the decreasing magnetic moment of the particles and the narrowing of the distorted region of the magnetic field near the core due to a decrease in spatial access for water protons. According to AFM, the bound Hsp70 layer leads to a 2-fold increase of the effective hydrodynamic diameter of MNP and, consequently, the magnetic shielding of the magnetic core for the water protons. Shielding of MNPs should cause a decrease in the relaxation rate r2m, as was shown in a long-term study of proton magnetic relaxation in suspensions of magnetic Hsp70 conjugates. Dextran-coated SPIONs showed slightly higher T_2 relaxivity than Hsp70 conjugates; however, this difference is not principal for contrast enhancement in MRI. The formation of an Hsp70 shell around SPION does not shield the magnetic core from water. Water protons perceive the influence of the magnetic field generated by cores of SPIONs coming close to the center due to intense diffusion and small proton size.

MRI of agar phantoms saturated by Hsp70-SPION conjugates also confirmed the high relaxivity of gel preparation. As a result of growth of relaxation under the influence of SPION-Hsp70, the phantom images have a view of dark spots with low NMR intensity. The magnetic characteristics of Hsp70-SPIONs obtained in vitro make it possible to use one as an effective contrast agent for MRI of the rat brain model in the case of sufficient biocompatibility and targeted accumulation in cancerous tissue. The observed rate of relaxation times was proportional to the Fe content in suspension. The intensity map of the MRI is known to depend on the distribution of T_1 and T_2 times associated with voxel position; therefore, the distribution of intensity NMR signal across the T_2--weighted images will evidence the potential accumulation of magnetic conjugate Hsp70-SPION in tumor cells. The measured relaxation characteristics of Hsp70-SPION conjugate in suspension remained constant in fractions after centrifugation and separation procedures on magnets. The stability and particle size of prepared SPIONs (<100 nm) are sufficient for in vivo MRI diagnostic experiments.

Biocompatibility of magnetic conjugate is another substantial demand for targeted delivery of drugs into brain tumors. The toxicology study shows that the Hsp70-SPION conjugates at diagnostic concentrations exert no toxicity toward C6 glioma cells. In vivo experiments also confirmed the safety of i.v. injections of SPIONs or Hsp70-SPION conjugates, as all of the animals survived the procedures and showed no signs of toxicity. Acute toxicity was not found for dose 0.01–1.6 mg/mouse SPION conjugates.[15] These data are in accordance with those of Hadjipanayis et al,[13] who studied the toxicity of the iron oxide nanoparticles on glioblastoma cells or normal human astrocytes and found no significant toxicity 3 days after treatment with nanoparticles. Biocompatible SPIONs were degraded and cleared from circulation by the endogenous iron metabolic pathways; iron content in blood revealed no difference from control after 2 weeks.

Biocompatible conjugates Hsp70 are not inert extracellular particles; the results point to the notable intracellular absorption. Our in vitro experiments demonstrated the incorporation of nanoparticles within C6 cell cytoplasm; the electron-dense Hsp70-SPION conjugates accumulated inside the endosome structures (Fig. 4). The possible mechanism of conjugate uptake is receptor-mediated endocytosis. Previously, several receptors for Hsp's were described on various cells, including scavenger receptors SR-A, SR-F1 (scavenger receptor class F–1/scavenger receptor expressed on endothelial cells–1), stabilin-1, and LOX-1[29–32]; c-type lectins such as Lectin-1, CD94, NKG2D, DC-SIGN[33–35]; receptor for α2 macroglobulin CD91[36]; and the Toll-like receptor (TLR-2, TLR-4) family.[37,38] In our study we assessed the other receptor for Hsp70, a member of the tumor necrosis factor receptor family, CD40, which is known to be expressed not only on antigen-presenting cells but also on glioma cells.[18–21,39] We observed a dramatic increase of CD40+ cells inside the glioma tumor in vivo (Fig. 3). We supposed that the microenvironment inside the tumor would drive the growth of the CD40 expression. In vitro, we modulated the oxidative stress and confirmed the hypothesis of the CD40 expression growth on the glioma cells under the stress stimuli (Supplementary material, Fig. S1). The redox status in the cell is determined by the balance of reactive oxygen and nitrogen species, free radicals such as superoxide (O_2), a hydroxyl radical (HO), and nonradicals that could generate free radicals (such as H_2O_2).[40] Previously it was shown that oxidative stress activates various pathways, including mitogen-activated protein kinase and response mediated by nuclear factor kappa-light-chain-enhancer of activated B cells (NF-κB), which mediate intracellular signal transduction.[41–43] It is believed that the activation of the NF-κB pathway in oxidative stress conditions promotes the expression of CD40 on the glioma cells[44]; CD40 was expressed in only the C6 glioma site but not in other normal brain areas. Conceivably, this could explain the preferential accumulation of fluorochrome-labeled Hsp70 inside the C6 glioma cells but not in the normal brain tissues when being i.v. administered to the tumor-bearing animal (Fig. 3). The presented data are in compliance with our previously obtained results when

Hsp70-containing hydrogel was applied on the surface of a 7-day-old B16F10 melanoma tumor. According to the histochemistry, Hsp70 diffused through the skin layer inside the B16 tumor.[45] As well as receptor-mediated cellular uptake of Hsp70, there have been other mechanisms described that could play a certain role in the Hsp70-SPION uptake, including anchoring to the lipid rafts.[46–48]

The cellular uptake of Hsp70 gives reason to assume that the notable accumulation of SPIONs conjugated with Hsp70 can be realized in glial tissue in vivo. Actually, the study demonstrated that Hsp70-SPION conjugate i.v. injected into a C6 rat glioma model accumulates in the tumors and enhances the contrast of their MRI images. The magnetic Hsp70 conjugate after i.v. injection was specifically delivered to malignant areas of implanted tumors (Fig. 5). According to the confocal microscopy data, we could observe the presence of nanoparticle aggregates within the cell cytoplasm or the extracellular space in the tumor site but not in the normal adjacent brain tissues (Fig. 5, right column). The presence of the SPIONs or Hsp70-SPIONs inside the glioma could be attributed to the destruction of the BBB, which is the main feature of malignant tumors.[49,50] Earlier it was shown that nanoparticles have the ability to cross the BBB, thus providing brain tumor targeting.[5,51,52] The case when the level of Hsp70-SPION retention in the glioma site was significantly higher compared with the nonconjugated SPIONs could be explained by the specific receptor-mediated endocytosis of the Hsp70-SPION conjugates by the CD40+ glioma cells. In favor of this are the in vitro data, where it was demonstrated (by means of confocal microscopy) that the magnitude of Hsp70-SPION uptake by C6 cells was higher than that of nonconjugated SPIONs (Fig. 4). The similar pattern of nanoparticle internalization (with a higher uptake of Hsp70-SPIONs in comparison with nonconjugated SPIONs) was observed in the case of HeLa cells (Supplementary material, Fig. S2). Hsp70-SPION conjugates show high relaxivity in the T_2-weighted regimen and can be used as negative contrast agents for MRI diagnostics of malignant tissues with overexpressed receptors for Hsp70. As a result of targeted delivery, the images become more enhanced with regard to resolution. The degree of negative contrast was comparable to that achieved by other contrast agents, including the earlier report of the EGFRvIII antibody conjugated with iron oxide nanoparticles.[13] The magnitude of the tumor accumulation of the Hsp70-SPIONs could be increased by the preliminary saturation of the Hsp receptors with i.v. injection of purified Hsp70 prior to the infusion of the Hsp70-SPION conjugates (Figs 5D and 6). We proposed that various receptors to the Hsp's, including Hsp70, exposed on different cells and mostly on the reticuloendothelial system cells,[16] thus contribute to receptor-mediated Hsp70-SPION internalization, affecting the accumulation inside the tumor tissue. Consequently, receptor saturation by the i.v. infusion of the purified Hsp70 could increase the retention of Hsp70-SPIONs inside the glioma. Previously, Binder et al[26] studied the saturation concentrations (varying from 0 to 200 μg/mL) for gp96, Hsp90, and Hsp70 with CD11b+ cells, and Hsp70 did not reach saturable binding at 200 μg/mL. According to our data, the accumulation of Hsp70–Alexa Fluor 555 conjugate inside the C6 glioma starts to be detectable at concentrations over 5 mg/kg (Fig. 3). Following i.v. treatment by purified Hsp70, we injected Hsp70-SPIONs and showed the dramatic increase of the hypointense zone in the tumor site on the T_2-weighted images compared with injection of conjugates without the preliminary saturation of the Hsp70 receptors (Fig. 5D).

In summary, the presented work shows the feasibility of glioma targeting by Hsp70-SPION conjugates via i.v. administration. The level of intratumoral accumulation is comparable to that of local infusion, which broadens the clinical application of these conjugates for targeted delivery to the metastatic or diffuse tumors and tumors located in eloquent brain areas. A possible way to further enhance the retention of a targeted Hsp70 drug at the malignant site is to focus Hsp70-SPIONs by a specially configured magnetic field via a magnet implant. Further steps for development of this targeted nanoconstruction include the improvement of stability, a pharmacokinetic study, and optimization of medical application.

Supplementary Material

Supplementary material is available at Neuro-Oncology Journal online (http://neuro-oncology.oxfordjournals.org/).

Funding

This study was supported by the grant of the Program of Russian Academy of Sciences (RAS) "Molecular and Cell Biology," grants of Russian Fund for Basic Research No 10-0401049 and No 11-08-00045, Governmental grant (20.11.2012) No 14.N08.11.0001.

Acknowledgments

Authors thank G. I. Stein and M. L. Vorobiev for the technical assistance in the confocal microscopy analysis. Authors are grateful to P. P. Klein for the preparation of illustrations.

Conflict of interest statement. None declared.

References

1. McCarthy JR, Weissleder R. Multifunctional magnetic nanoparticles for targeted imaging and therapy. *Adv Drug Deliv Rev*. 2008;60:1241–1251.
2. Wankhede M, Bouras A, Kaluzova M, Hadjipanayis CG. Magnetic nanoparticles: an emerging technology for malignant brain tumor imaging and therapy. *Expert Rev Clin Pharmacol*. 2012;5:173–186.
3. Salloum M, Ma R, Zhu L. Enhancement in treatment planning for magnetic nanoparticle hyperthermia: optimization of the heat absorption pattern. *Int J Hyperthermia*. 2009;25:309–321.
4. Kobayashi T. Cancer hyperthermia using magnetic nanoparticles. *Biotechnol J*. 2011;6:1342–1347.
5. Jordan A, Scholz R, Maier-Hauff K, et al. The effect of thermotherapy using magnetic nanoparticles on rat malignant glioma. *J Neurooncol*. 2006;78:7–14.
6. Ren Y, Zhang H, Chen B, et al. Multifunctional magnetic Fe_3O_4 nanoparticles combined with chemotherapy and hyperthermia to overcome multidrug resistance. *Int J Nanomedicine*. 2012;7:2261–2269.
7. Basel M, Balivada S, Wang H, et al. Cell-delivered magnetic nanoparticles caused hyperthermia-mediated increased survival in a murine pancreatic cancer model. *Int J Nanomedicine*. 2012;7:297–306.

8. Johannsen M, Gneveckow U, Taymoorian K, et al. Morbidity and quality of life during thermotherapy using magnetic nanoparticles in locally recurrent prostate cancer: results of a prospective phase I trial. *Int J Hyperthermia*. 2007;23:315–323.
9. Maier-Hauff K, Rothe R, Scholz R, et al. Intracranial thermotherapy using magnetic nanoparticles combined with external beam radiotherapy: results of a feasibility study on patients with glioblastoma multiforme. *J Neurooncol*. 2007;81:53–60.
10. Maier-Hauff K, Ulrich F, Nestler D, et al. Efficacy and safety of intratumoral thermotherapy using magnetic iron-oxide nanoparticles combined with external beam radiotherapy on patients with recurrent glioblastoma multiforme. *J Neurooncol*. 2011;103(2):317–324.
11. Stupp R, Hegi ME, Mason WP, et al. Effects of radiotherapy with concomitant and adjuvant temozolomide versus radiotherapy alone on survival in glioblastoma in a randomized phase III study: 5-year analysis of the EORTC-NCIC trial. *Lancet Oncol*. 2009;10:459–466.
12. Gupta AK, Gupta M. Synthesis and surface engineering of iron oxide nanoparticles for biomedical applications. *Biomaterials*. 2005; 26:3995–4021.
13. Hadjipanayis CG, Machaidze R, Kaluzova M, et al. EGFRvIII antibody conjugated iron oxide nanoparticles for MRI guided convection-enhanced delivery and targeted therapy of glioblastoma. *Cancer Res*. 2010;70:6303–6312.
14. Chen BA, Cheng J, Shen MF, et al. Magnetic nanoparticle of Fe_3O_4 and 5-bromotetrandrin interact synergistically to induce apoptosis by daunorubicin in leukemia cells. *Int J Nanomedicine*. 2009;4:65–71.
15. Nikolaev BP, Marchenko YY, Yakovleva LY, et al. Magnetic epidermal growth factor for targeted delivery to grafted tumor in mouse model. *IEEE Trans Magn*. 2013;49:1–7.
16. Calderwood SK, Theriault JR, Gong J. Message in a bottle: role of the 70 kDa HSP in anti-tumor immunity. *Eur J Cancer*. 2005;35:2518–2527.
17. Calderwood SK, Stevenson MA, Murshid A. Heat shock proteins, autoimmunity, and cancer treatment. *Autoimmune Dis*. 2012;2012: 486069.
18. Murshid A, Gong J, Calderwood SK. The role of heat shock proteins in antigen cross presentation. *Front Immunol*. 2012;3:63.
19. Wischhusen J, Schneider D, Mittelbronn M, et al. Death receptor-mediated apoptosis in human malignant glioma cells: modulation by the CD40/CD40L system. *J Neuroimmunol*. 2005;162: 28–42.
20. Zhang Y, Huang T, Hu Y, Wang Y. Activation of CD40 by soluble recombinant human CD40 ligand inhibits human glioma cells proliferation via nuclear factor-κB signaling pathway. *J Huazhong Univ Sci Technolog Med Sci*. 2012;32:691–696.
21. Tewari R, Choudhury SR, Mehta VS, Sen E. TNFα regulates the localization of CD40 in lipid rafts of glioma cells. *Mol Biol Rep*. 2012; 39:8695–8699.
22. Srivastava PK, Callahan MK, Mauri MM. Treating human cancers with heat shock protein–peptide complexes: the road ahead. *Expert Opin Biol Ther*. 2009;9:179–186.
23. Ito A, Matsuoka F, Honda H, Kobayashi T. Antitumor effects of combined therapy of recombinant heat shock protein 70 and hyperthermia using magnetic nanoparticles in an experimental subcutaneous murine melanoma. *Cancer Immunol Immunother*. 2004;53:26–32.
24. Massart R. Preparation of aqueous magnetic liquids in alkaline and acidic media. *IEEE Trans Magn*. 1981;17:1247–1248.
25. Lazarev VF, Onokhin KV, Antimonova OI, et al. Kinetics of chaperone activity of proteins Hsp70 and Hdj1 in human leukemia U937 cells after preconditioning with thermal shock or compound U133. *Biochemistry (Moscow)*. 2011;76:590–595.
26. Binder RJ, Harris ML, Menoret A, Srivastava PK. Saturation, competition, and specificity in interaction of heat shock proteins (hsp) gp96, hsp90, and hsp70 with $CD11b^+$ Cells. *J Immunol*. 2000;165:2582–2587.
27. Zhou J, Tryggestad E, Wen Z, et al. Differentiation between glioma and radiation necrosis using molecular magnetic resonance imaging of endogenous proteins and peptides. *Nat Med*. 2011;17:130–134.
28. Rosen JE, Chan L, Shieh DB, Gu FX. Iron oxide nanoparticles for targeted cancer imaging and diagnostics. *Nanomedicine*. 2012;8:275–290.
29. Murshid A, Gong J, Calderwood SK. Heat shock protein 90 mediates efficient antigen cross-presentation through the scavenger receptor expressed by endothelial cells–I. *J Immunol*. 2010;185:2903–2917.
30. Calderwood SK, Theriault J, Gray PJ, Gong J. Cell surface receptors for molecular chaperones. *Methods*. 2007;43:199–206.
31. Delneste Y, Magistrelli G, Gauchat J, et al. Involvement of LOX-1 in dendritic cell–mediated antigen cross-presentation. *Immunity*. 2002;17:353–362.
32. Theriault JR, Adachi H, Calderwood SK. Role of scavenger receptors in the binding and internalization of heat shock protein 70. *J Immunol*. 2006;177:8604–8611.
33. Pegram HJ, Andrews DM, Smyth MJ, Darcy PK, Kershaw MH. Activating and inhibitory receptors of natural killer cells. *Immunol Cell Biol*. 2010; 89:216–224.
34. Graham LM, Brown GD. The Dectin-2 family of C-type lectins in immunity and homeostasis. *Cytokine*. 2009;48:148–155.
35. den Dunnen J, Gringhuis SI, Geijtenbeek TB. Innate signaling by the C-type lectin DC-SIGN dictates immune responses. *Cancer Immunol Immunother*. 2009;58:1149–1157.
36. Basu S, Binder RJ, Ramalingam T, Srivastava PK. CD91 is a common receptor for heat shock proteins Gp96, Hsp90, Hsp70, and calreticulin. *Immunity*. 2001;14:303–313.
37. Asea A, Kraeft SK, Kurt-Jones EA, et al. HSP70 stimulates cytokine production through a CD14-dependant pathway, demonstrating its dual role as a chaperone and cytokine. *Nat Med*. 2000;6:435–442.
38. Vabulas RM, Ahmad-Nejad P, Ghose S, et al. HSP70 as endogenous stimulus of the Toll/interleukin-1 receptor signal pathway. *J Biol Chem*. 2002;277:15107–15112.
39. Becker T, Hartl FU, Wieland F. CD40, an extracellular receptor for binding and uptake of Hsp70–peptide complexes. *J Cell Biol*. 2002;158: 1277–1285.
40. Kamata H, Honda S, Maeda S, Chang L, Hirata H, Karin M. Reactive oxygen species promote TNFalpha-induced death and sustained JNK activation by inhibiting MAP kinase phosphatases. *Cell*. 2005;120(5): 649–661.
41. Kratsovnik E, Bromberg Y, Sperling O, Zoref-Shani E. Oxidative stress activates transcription factor NF-kB–mediated protective signaling in primary rat neuronal cultures. *J Mol Neurosci*. 2005;26(1):27–32.
42. Nakano H, Nakajima A, Sakon-Komazawa S, Piao JH, Xue X, Okumura K. Reactive oxygen species mediate crosstalk between NF-kappaB and JNK. *Cell Death Differ*. 2006;13(5):730–737.
43. Temkin V, Karin M. From death receptor to reactive oxygen species and cJun N-terminal protein kinase: the receptor-interacting protein 1 odyssey. *Immunol Rev*. 2007;220(1):8–21.
44. Qin H, Wilson CA, Lee SJ, Zhao X, Benveniste EN. LPS induces CD40 gene expression through the activation of NF-κB and STAT-1α in macrophages and microglia. *Blood*. 2005;106:3114–3122.
45. Abkin SV, Pankratova KM, Komarova EY, Guzhova IV, Margulis BA. Hsp70 chaperone-based gel composition as a novel immunotherapeutic anti-tumor tool. *Cell Stress Chaperones*. 2013;18:391–396.

46. Triantafilou M, Miyake K, Golenbock DT, Triantafilou K. Mediators of innate immune recognition of bacteria concentrate in lipid rafts and facilitate lipopolysaccharide-induced cell activation. *J Cell Sci*. 2002; 115:2603–2611.
47. Broquet AH, Thomas G, Masliah J, Trugnan G, Bachelet M. Expression of the molecular chaperone Hsp70 in detergent-resistant microdomains correlates with its membrane delivery and release. *J Biol Chem*. 2003; 278:21601–21606.
48. Gehrmann M, Liebisch G, Schmitz G, et al. Tumor-specific hsp70 plasma membrane localization is enabled by the glycosphingolipid Gb3. *PLoS One*. 2008;3(4):e1925.
49. Vajkoczy P, Menger MD. Vascular microenvironment in gliomas. *J Neurooncol*. 2000;50:99–108.
50. Batchelor TT, Sorensen AG, di Tomaso E, et al. AZD2171, a pan-VEGF receptor tyrosine kinase inhibitor, normalizes tumor vasculature and alleviates edema in glioblastoma patients. *Cancer Cell*. 2007;11:83–95.
51. Chertok B, Moffat BA, David AE, et al. Iron oxide nanoparticles as a drug delivery vehicle for MRI monitored magnetic targeting of brain tumors. *Biomaterials*. 2008;29:487–496.
52. Agemy L, Friedmann-Morvinski D, Kotamraju VR, et al. Targeted nanoparticle enhanced proapoptotic peptide as potential therapy for glioblastoma. *Proc Natl Acad Sci U S A*. 2011;108:17450–17455.